



The following Communications have been judged by at least two referees to be “very important papers” and will be published online at www.angewandte.org soon:

Y. H. Kim, S. Banta*

Complete Oxidation of Methanol in an Enzymatic Biofuel Cell by a Self-Assembling Hydrogel Created from Three Modified Dehydrogenases

R. M. Culik, A. L. Serrano, M. R. Bunagan,* F. Gai*

Achieving Secondary Structural Resolution in Kinetic Measurements of Protein Folding: A Case Study of the Folding Mechanism of Trp-cage



Chemistry, Science, and Our Sustainable Future

Editorial

Y. T. Lee,* A. W.-C. Yang – 10260–10261



“Science is fun because it provides a life-long satisfaction of curiosity.

My favorite time of day is dinner (for several reasons) ...”

This and more about Jurriaan Huskens can be found on page 10282.

Author Profile

Jurriaan Huskens ————— 10282



H. Bayley



J. W. Goodby



C. P. Grey



I. Manners

News

New Fellows Elected to The Royal Society: H. Bayley, J. W. Goodby,

C. P. Grey, I. Manners ————— 10283

Obituaries

F. Gordon A. Stone (1925–2011)

A. F. Hill ————— 10284–10285

Books

Chemistry in Space

Dieter Rehder

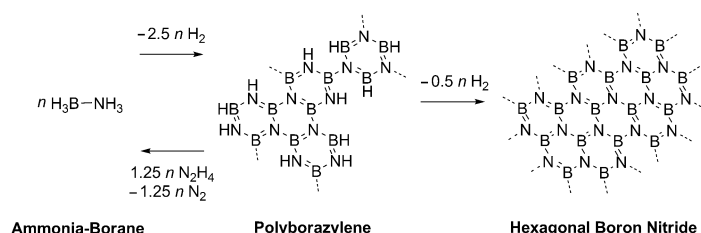
reviewed by C. Streb ————— 10286

Highlights

Boron–Nitrogen Compounds

G. R. Whittell,
I. Manners* — 10288 – 10289

Advances with Ammonia-Borane:
Improved Recycling and Use as a
Precursor to Atomically Thin BN Films



BN working: Under ambient conditions, ammonia-borane (AB) dehydrogenates to polyborazylene, which, in a recent advance, can be readily regenerated in a key step for hydrogen-storage applications

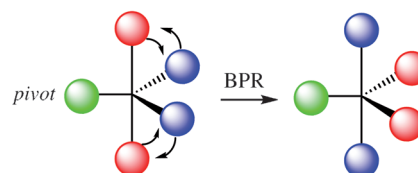
(see scheme). In contrast, recent reports show that dehydrogenation of AB under chemical vapor deposition conditions yields atomically thin films of hexagonal BN and their hybrids with graphene.

Pseudorotation

C. Moberg* — 10290 – 10292

Stereomutation in Trigonal-Bipyramidal
Systems: A Unified Picture

Same difference: Berry pseudorotation (BPR) and Ugi turnstile rotation, which are generally treated as two distinctly different mechanisms for rearrangement of trigonal-bipyramidal structures, have been shown to be equivalent. Alternative mechanisms consist of sequences of pseudorotations proceeding in a single step.

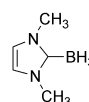
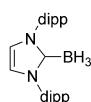


Reviews

NHC-Boranes

D. P. Curran,* A. Solov'yev,
M. Makhoulouf Brahmi, L. Fensterbank,*
M. Malacria, E. Lacôte* — 10294 – 10317

NHC-borane reagents, reactants, and...reactive intermediates



NHC-BH₂⁺

NHC-BH₂[•]

NHC-BH₂⁻



Synthesis and Reactions of N-Heterocyclic
Carbene Boranes

Forget everything you know about boron chemistry ... NHC-boranes (see picture) are different. Functionalities that are not usually present in organoboron compounds can be easily introduced. New classes of rare boron-based reactive

intermediates (cations, radicals, and anions) have emerged. And NHC-boranes are promising as reagents and catalysts in organic synthesis and as co-initiators in radical polymerization.

For the USA and Canada:
ANGEWANDTE CHEMIE International
Edition (ISSN 1433-7851) is published weekly
by Wiley-VCH, PO Box 191161, 69451 Wein-
heim, Germany. Air freight and mailing in the
USA by Publications Expediting Inc., 200
Meacham Ave., Elmont, NY 11003. Periodicals

postage paid at Jamaica, NY 11431. US POST-
MASTER: send address changes to *Angewandte
Chemie*, Journal Customer Services, John
Wiley & Sons Inc., 350 Main St., Malden,
MA 02148-5020. Annual subscription price for
institutions: US\$ 11,738/10,206 (valid for print
and electronic / print or electronic delivery); for

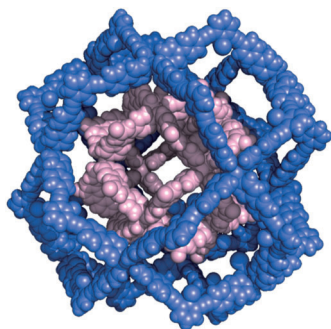
individuals who are personal members of a
national chemical society prices are available
on request. Postage and handling charges
included. All prices are subject to local VAT/
sales tax.

Communications

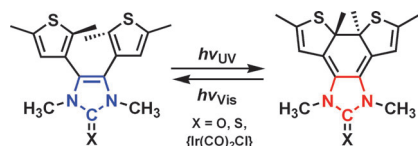
Self-Assembly

Q.-F. Sun, T. Murase, S. Sato,
 M. Fujita* _____ 10318–10321

A Sphere-in-Sphere Complex by
 Orthogonal Self-Assembly



Russian dolls: Two covalently tethered, curved bispyridinyl ligands and Pd^{II} ions have been shown to self-assemble into a sphere-in-sphere complex (6.3 nm in diameter; see X-ray structure). The two ligands did not form heteroleptic mixed complexes, but instead assembled into two distinct homogeneous [M₁₂L₂₄] cuboctahedra, reminiscent of a double-shell viral capsid.

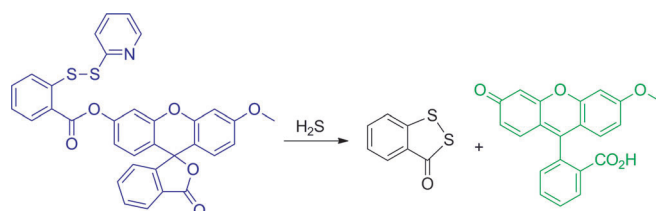


Ligands in the limelight: Light was used to change the electron-donating properties of an N-heterocyclic carbene (NHC) moiety within chalcogen and metal adducts. Photoinduced electrocyclic ring closure of a photochromic 4,5-dithienyl-imidazolone increased its ν_{CO} frequency. Likewise, UV irradiation of an analogous photochromic [(NHC)Ir(CO)₂Cl] complex decreased the carbene's electron-donating ability. Subsequent exposure to visible light reversed both photocyclization reactions.

Photoswitches

B. M. Neilson, V. M. Lynch,
 C. W. Bielawski* _____ 10322–10326

Photoswitchable N-Heterocyclic
 Carbenes: Using Light to Modulate
 Electron-Donating Properties



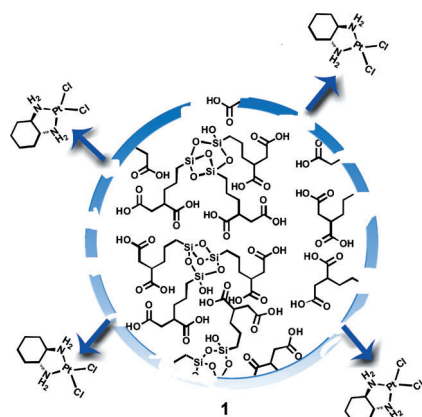
Reaction-based sensing: A fluorescent probe for the detection of hydrogen sulfide was prepared and evaluated on the basis of H₂S-mediated benzodithioline

formation. The probe showed good selectivity and sensitivity for hydrogen sulfide.

Sensors

C. Liu, J. Pan, S. Li, Y. Zhao, L. Y. Wu,
 C. E. Berkman, A. R. Whorton,
 M. Xian* _____ 10327–10329

Capture and Visualization of Hydrogen
 Sulfide by a Fluorescent Probe



Trigger happy: Polylsilsesquioxane (PSQ) nanoparticles that contain a Pt^{IV}-based active agent (**1**; see picture) can be used for the triggered delivery of chemotherapeutics. The cytotoxicity of **1** was superior to that of oxaliplatin against four cancer cell lines in vitro, and targeting further enhanced the cytotoxicity. PEGylated and anisamide-targeted **1** showed drastically superior efficacy to oxaliplatin in inhibiting tumor growth.

Antitumor Agents

J. Della Rocca, R. C. Huxford,
 E. Comstock-Duggan,
 W. Lin* _____ 10330–10334

Polylsilsesquioxane Nanoparticles for
 Targeted Platin-Based Cancer
 Chemotherapy by Triggered Release

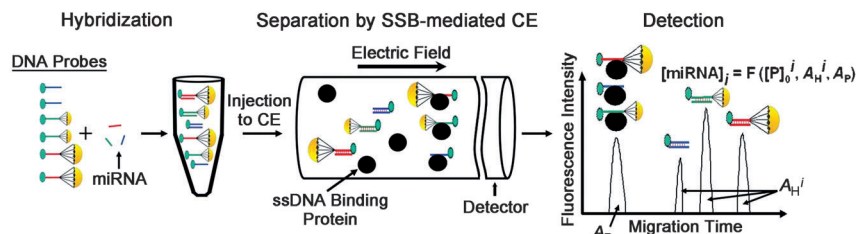


miRNA Detection

D. W. Wegman,
S. N. Krylov* — 10335 – 10339



Direct Quantitative Analysis of Multiple miRNAs (DQAMmiR)



Dragging it out: The first direct quantitative analysis of multiple miRNAs (DQAMmiR) uses miRNAs directly, without chemical or enzymatic modification, and accurately determines concentrations of multiple miRNAs without the need for

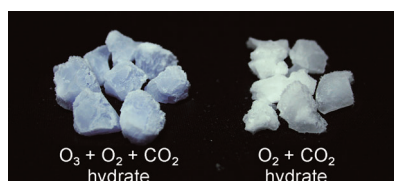
calibration curves. This method involves a capillary-electrophoresis-based hybridization assay with a combination of two separation-enhancement approaches: drag tags and single strand DNA binding protein (SSB).

Ozone-Containing Hydrates

T. Nakajima, S. Akatsu, R. Ohmura,
S. Takeya, Y. H. Mori* — 10340 – 10343



Molecular Storage of Ozone in a Clathrate Hydrate Formed from an $O_3 + O_2 + CO_2$ Gas Mixture



Ozone in the rocks: A clathrate hydrate can be formed from an $O_3 + O_2 + CO_2$ gas mixture (see picture, left; $O_2 + CO_2$ hydrate is shown for comparison). The pale blue color of the former is probably due to the ozone molecules encaged within. The $O_3 + O_2 + CO_2$ hydrate stored in air at normal pressure at $-25^\circ C$ can preserve ozone (0.1% in mass fraction) for over four weeks.

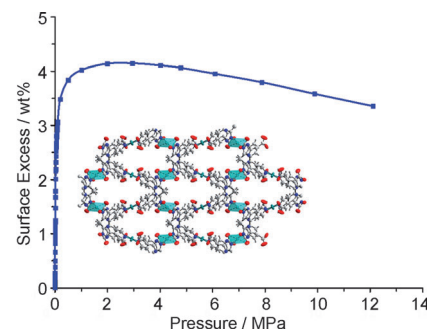
Microporous MOFs

D. Lässig, J. Lincke, J. Moellmer,
C. Reichenbach, A. Moeller, R. Gläser,
G. Kalies, K. A. Cychosz, M. Thommes,
R. Staudt,
H. Krautscheid* — 10344 – 10348



A Microporous Copper Metal–Organic Framework with High H_2 and CO_2 Adsorption Capacity at Ambient Pressure

Fully accessible: Uptakes of 9.2 mmol g^{-1} (40.5 wt%) for CO_2 at 273 K/0.1 MPa and $15.23 \text{ mmol g}^{-1}$ (3.07 wt%) for H_2 at 77 K/0.1 MPa are among the highest reported for metal–organic frameworks (MOFs) and are found for a novel, highly microporous copper-based MOF (see picture; Cu turquoise, O red, N blue). Thermal analyses show a stability of the flexible framework up to $250^\circ C$.



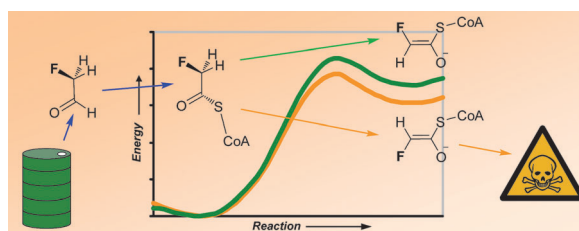
Enzyme Stereospecificity



M. W. van der Kamp, J. D. McGeagh,
A. J. Mulholland* — 10349 – 10351

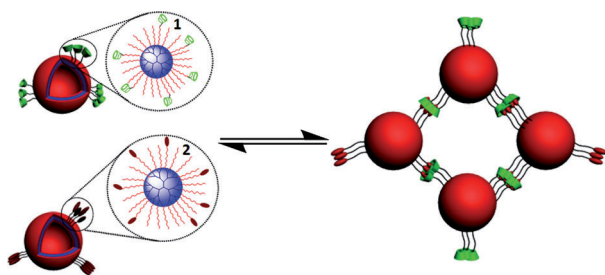


“Lethal Synthesis” of Fluorocitrate by Citrate Synthase Explained through QM/MM Modeling



A classic example of enzyme stereospecificity is the title reaction involving the enantioselective conversion of fluoroacetyl-CoA. High-level modeling of the enzyme reaction shows that preferential formation of an *E*-enolate explains the

experimentally observed specificity. The results indicate that selectivity is primarily a result of the inherent energy difference between the *E*- and *Z*-enolates of fluoroacetyl-CoA.



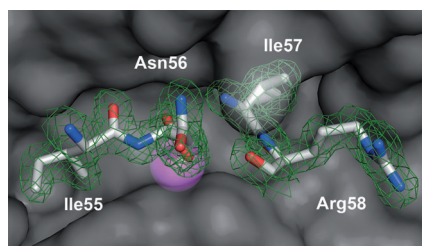
Sleeping giants: As a mimic of cell agglomeration to form tissues, a novel vesicle aggregation process with the characteristic advantages of being highly efficient, light-responsive, reversible, large-scale, and stable is reported. Giant

hyperbranched polymer vesicles (5–10 μm) are used as the building blocks (see scheme), and the vesicle aggregates can assemble and disassemble with alternating UV and Vis irradiation.

Vesicles

H. Jin, Y. Zheng, Y. Liu, H. Cheng, Y. Zhou,* D. Yan — 10352 – 10356

Reversible and Large-Scale Cytomimetic Vesicle Aggregation: Light-Responsive Host–Guest Interactions



It goes both ways: An unprecedented mechanism of metalloendopeptidase inhibition has been identified for the insect metalloproteinase inhibitor, which is both cleaved and rejoined at bond Asn56–Ile57 by thermolysin under appropriate conditions. A two-product complex is formed after hydrolysis and, simultaneously, a Michaelis complex is poised for synthesis of a peptide bond (see crystal structure).

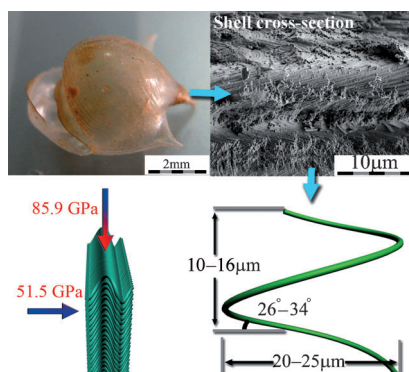
Peptide-Bond Synthesis

J. L. Arolas, T. O. Botelho, A. Vilcinskis, F. X. Gomis-Rüth* — 10357 – 10360

Structural Evidence for Standard-Mechanism Inhibition in Metallopeptidases from a Complex Poised to Resynthesize a Peptide Bond



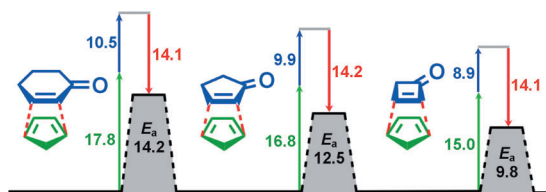
Natural ultrathin flexible armor: Novel hierarchical microstructures composed of densely packed helical aragonite nanofibers were observed in an ultrathin pteropod shell by a combination of techniques. The helical nanofibers are interlocked and crystallographically aligned with a misorientation of up to 10° . These structural features may contribute to its advanced anisotropic mechanical properties.



Biomaterialization

T. Zhang, Y. Ma,* K. Chen, M. Kunz, N. Tamura, M. Qiang, J. Xu, L. Qi* — 10361 – 10365

Structure and Mechanical Properties of a Pteropod Shell Consisting of Interlocked Helical Aragonite Nanofibers



Quantum chemical calculations are used to investigate the experimentally measured reactivities of cyclic dienes and cycloalkenones in the Diels–Alder reaction. The interaction energies (red) are

nearly constant; differences arise in changes in distortion energies of both dienophile (blue) and diene (green; see picture, E_a = activation energy; values in kcal mol^{-1}).

Cycloaddition

R. S. Paton,* S. Kim, A. G. Ross, S. J. Danishefsky, K. N. Houk* — 10366 – 10368

Experimental Diels–Alder Reactivities of Cycloalkenones and Cyclic Dienes Explained through Transition-State Distortion Energies

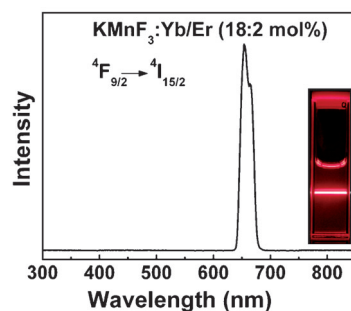


Upconversion

J. Wang, F. Wang, C. Wang, Z. Liu,
X. Liu* 10369–10372



Single-Band Upconversion Emission in Lanthanide-Doped KMnF₃ Nanocrystals



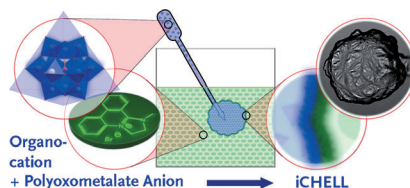
Clear sight: The upconversion emission spectra of KMnF₃ nanocrystals co-doped with Yb/Er (18:2 mol%; see picture) and Yb/Ho (18:2 mol%) reveal strong single-band emissions. The application of this pure, single-band emission for deep-tissue imaging is demonstrated.

Inorganic Chemical Cells

G. J. T. Cooper, P. J. Kitson, R. Winter,
M. Zagnoni, D.-L. Long,
L. Cronin* 10373–10376



Modular Redox-Active Inorganic Chemical Cells: iCHELLs



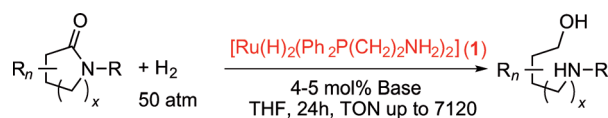
Cell within a cell: Interfacial membrane formation by cation exchange of polyoxo-metalates produces modular inorganic chemical cells with tunable morphology, properties, and composition (see picture). These inorganic chemical cells (iCHELLs), which show redox activity, chirality, as well as selective permeability towards small molecules, can be nested within one another, potentially allowing stepwise reactions to occur in sequence within the cell.

Homogeneous Catalysis

J. M. John,
S. H. Bergens* 10377–10380



A Highly Active Catalyst for the Hydrogenation of Amides to Alcohols and Amines



Amide-zing: The reaction between 2 equivalents of Ph₂P(CH₂)₂NH₂ and *cis*-[Ru(CH₃CN)₂(η³-C₃H₅)(cod)]BF₄ (cod = 1,5-cyclooctadiene) forms a highly active catalyst precursor for the selective hydrogenation of amides. The reaction proceeds with excellent atom economy, yield,

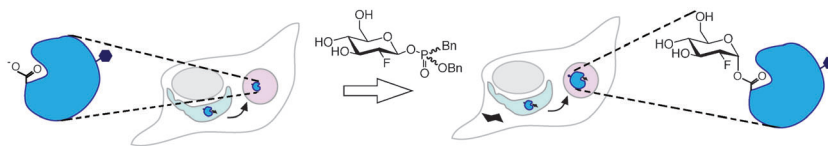
and turnover numbers (TONs) under moderate reaction conditions. The technology offers a greener, practical approach to the use of metal hydride reagents commonly employed in both academia and industry.

Enzyme Inhibition

B. P. Rempel, M. B. Tropak,
D. J. Mahuran,
S. G. Withers* 10381–10383

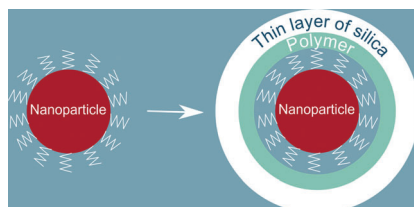


Tailoring the Specificity and Reactivity of a Mechanism-Based Inactivator of Glucocerebrosidase for Potential Therapeutic Applications



Chaperoning an enzyme: Fluorosugar glycosidase inactivators with tunable phosphorus-based leaving groups react quickly with the catalytic nucleophile in β glucocerebrosidase (blue circle; Bn = benzyl). In Western blot analysis, Gaucher

patient cells treated with these inactivators show increased intracellular levels of mutant enzyme, presumably because of increased transit from the endoplasmic reticulum (pale blue) to the lysosome (pale pink).

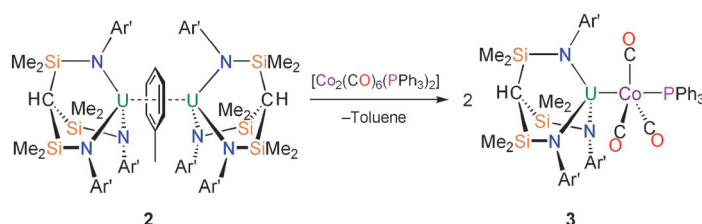


Doubly capped nanocrystals: A new technique was developed for coating of colloidal inorganic nanoparticles with different surface properties with a thin, cross-linked, and functionalized shell containing organic and inorganic layers (see picture). The underlying amphiphilic polymer foundation arranges on the particle surface as predicted in past reports.

Organic–Inorganic Hybrid Composites

P. D. McNaughter, J. C. Bear, D. C. Steytler, A. G. Mayes, T. Nann* — 10384–10387

A Thin Silica–Polymer Shell for Functionalizing Colloidal Inorganic Nanoparticles



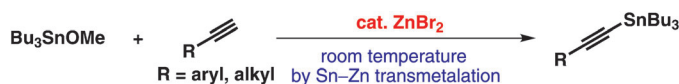
U–Co bond: Reduction of $[\text{U}(\text{Ts}^{\text{xy}})(\text{Cl})-(\text{thf})]$ [**1**; $\text{Ts}^{\text{xy}} = \text{HC}(\text{SiMe}_2\text{NAr})_3$; $\text{Ar} = 3,5\text{-Me}_2\text{C}_6\text{H}_3$] with KC_8 in toluene afforded the new arene-bridged diuranium complex **2**, whereas reduction of **1** in aliphatic hydrocarbons resulted in C–N bond activation and formation of an imido-aryl

complex, which exhibits an unusual ferromagnetic interaction between the two uranium centers. The synthetic utility of **2** was demonstrated by the first synthesis of a U–Co complex, $[\text{U}(\text{Ts}^{\text{xy}})\text{Co}(\text{CO})_3(\text{PPh}_3)]$ (**3**).

Uranium Arenes

D. Patel, F. Moro, J. McMaster, W. Lewis, A. J. Blake, S. T. Liddle* — 10388–10392

A Formal High Oxidation State Inverse-Sandwich Diuranium Complex: A New Route to f-Block-Metal Bonds



Metal hopping: Various alkynylstannanes were synthesized by the direct reaction of Bu_3SnOMe with terminal alkynes at room temperature in the presence of a ZnBr_2

catalyst. Rather than acting as a Lewis acid, ZnBr_2 was transmetalated with Bu_3SnOMe to give $\text{Zn}(\text{OMe})_2$, which is key to the catalytic reaction.

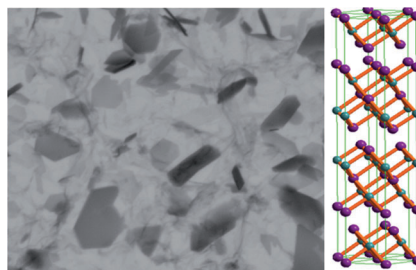
Stannanes

K. Kiyokawa, N. Tachikake, M. Yasuda, A. Baba* — 10393–10396

Direct Synthesis of Alkynylstannanes: ZnBr_2 Catalyst for the Reaction of Tributyltin Methoxide and Terminal Alkynes



Bi_2Te_3 nanosheets have been synthesized on Si substrates by surface-assisted chemical vapor transport. The crumpled Bi_2Te_3 sheets grow in the basal plane of the hexagonal structure and are typically ≤ 3 nm in thickness (see picture; Te purple, Bi green). Raman studies found that modes involving atom displacement along the c axis that are inactive in the bulk material become Raman-active in the Bi_2Te_3 nanosheets.



Nanosheets

Y. Zhao, R. W. Hughes, Z. Su, W. Zhou, D. H. Gregory* — 10397–10401

One-Step Synthesis of Bismuth Telluride Nanosheets of a Few Quintuple Layers in Thickness



Cross-Coupling

X. Qian, A. Auffrant, A. Felouat,
C. Gosmini* 10402 – 10405



Cobalt-Catalyzed Reductive Allylation of Alkyl Halides with Allylic Acetates or Carbonates



LG = OCOMe, OCO₂Me

An efficient method for the direct allylation of alkyl halides catalyzed by simple cobalt(II) bromide has been developed. This reaction, using a variety of substi-

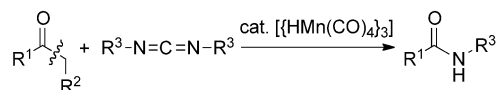
tuted allylic acetates or carbonates, provides the linear product as the major product. It displays broad substrate scope and good functional group tolerance.

C–C Cleavage

Y. Kuninobu,* T. Uesugi, A. Kawata,
K. Takai* 10406 – 10408



Manganese-Catalyzed Cleavage of a Carbon–Carbon Single Bond between Carbonyl Carbon and α -Carbon Atoms of Ketones



Singled out: Treatment of ketones with carbodiimides in the presence of a catalytic amount of either $[\{\text{HMn}(\text{CO})_4\}_3]$ or $[\text{Mn}_2(\text{CO})_{10}]$ gave amides in good to excellent yields. In this reaction, the

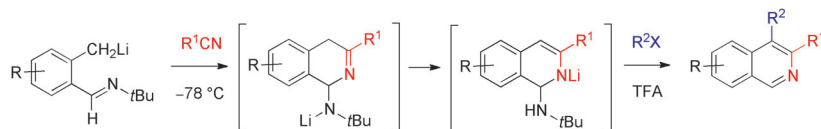
carbon–carbon single bond of a ketone is cleaved efficiently. The reaction also proceeded by using isocyanates instead of carbodiimides.

Synthetic Methods

C. Si, A. G. Myers* 10409 – 10413



A Versatile Synthesis of Substituted Isoquinolines



Lithiated o-tolualdehyde tert-butylimines were shown to condense with nitriles to form eneamido anion intermediates that were trapped in situ with various electrophiles, thus affording a diverse array of highly substituted isoquinolines, many of

which are difficult to access by known methods. Further substitutional diversification was achieved by modification of the work-up conditions and by subsequent transformations.

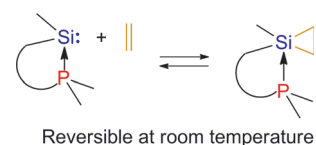
Siliranes

R. Rodriguez, D. Gau, T. Kato,*
N. Saffon-Merceron, A. De C  zar,
F. P. Coss  o,
A. Baceiredo* 10414 – 10416



Reversible Binding of Ethylene to Silylene–Phosphine Complexes at Room Temperature

On and off: The concerted [2+1] cycloaddition reaction of phosphine–silylene complexes with ethylene affords the corresponding pentacoordinate siliranes. The conversion is strongly related to the ethylene pressure, and the reaction is reversible at room temperature. The structure of one silirane was determined by X-ray diffraction analysis.



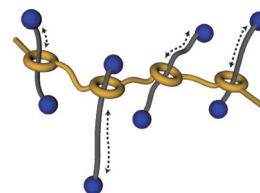
Supramolecular Polymers

Y. Kohsaka, Y. Koyama,
T. Takata* 10417 – 10420

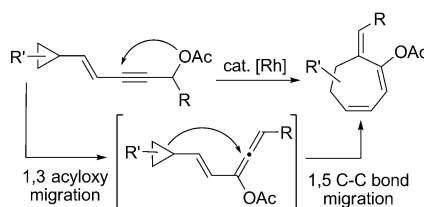


Graft Polyrotaxanes: A New Class of Graft Copolymers with Mobile Graft Chains

The synthesis and structure of graft polyrotaxane, a novel class of graft copolymer possessing mobile graft chains, is described. Poly(tetrahydrofuran) was bound to the axle components of pseudo[2]rotaxane as the graft chain by a grafting-onto method to afford the corresponding graft polyrotaxane (see picture). *N*-Acetylation of the ammonium moieties lead to an increase in the dynamic radius of the graft polyrotaxane.



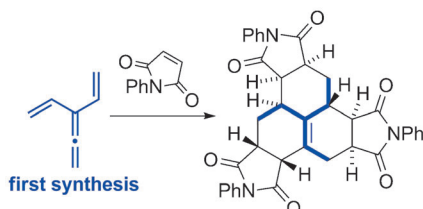
The golden side of rhodium: Highly functionalized seven-membered rings were prepared from substituted cyclopropanes by a Rh^I-catalyzed tandem isomerization reaction. The π -acidic Rh^I catalyst promoted the formation of an allene intermediate by a 1,3 acyloxy migration of a propargyl ester and a subsequent net 1,5 migration of a cyclopropane C–C bond.



Ring Expansion

X. Li, M. Zhang, D. Shu, P. J. Robichaux, S. Huang, W. Tang* — 10421 – 10424

Rhodium-Catalyzed Ring Expansion of Cyclopropanes to Seven-membered Rings by 1,5 C–C Bond Migration



first synthesis

- unprecedented triple cycloaddition sequence
- six C–C bonds
- three rings
- eight stereocenters
- high diastereoselectivity

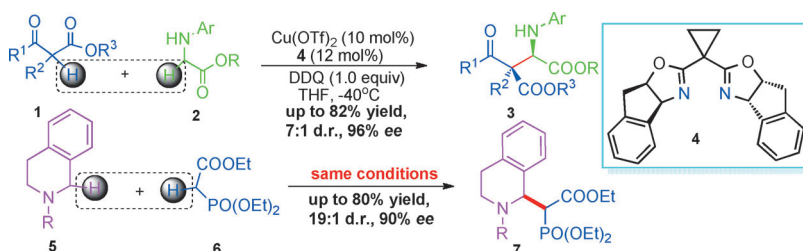
How to hit a triple: The title hydrocarbon, one of the most π -bond-rich small molecules, has been synthesized and characterized for the first time. This highly reactive hydrocarbon undergoes a new

diene-transmissive, triple Diels–Alder cycloaddition sequence to form six new C–C bonds and the fused tricyclic phenylene ring system in one step. Controlled single additions have also been achieved.

π -Bond-Rich Hydrocarbons

K. M. Cergol, C. G. Newton, A. L. Lawrence, A. C. Willis, M. N. Paddon-Row,* M. S. Sherburn* — 10425 – 10428

1,1-Divinylallene



Simple and efficient: A one-pot oxidative and catalytic enantioselective alkylation of α -C_{sp³}-H bonds adjacent to a nitrogen atom was realized for the first time. This novel strategy provides a simple, efficient,

and environmentally friendly access to diverse optically active α -alkyl α -amino acid and C1-alkylated tetrahydroisoquinoline derivatives.

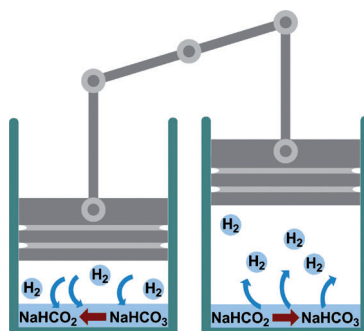
C–H Activation

G. Zhang, Y. Zhang, R. Wang* — 10429 – 10432

Catalytic Asymmetric Activation of a C_{sp³}-H Bond Adjacent to a Nitrogen Atom: A Versatile Approach to Optically Active α -Alkyl α -Amino Acids and C1-Alkylated Tetrahydroisoquinoline Derivatives



Soda stream: Sodium bicarbonate was cyclically hydrogenated in aqueous solution to sodium formate at 100 bar H₂ in the presence of a Ru^{II}-sulfonated phosphine catalyst. The system functions as a true charge/discharge device for storage and delivery of hydrogen without the need for isolation of either formate or bicarbonate.



Hydrogen Storage

G. Papp,* J. Csorba, G. Laurenczy, F. Joó* — 10433 – 10435

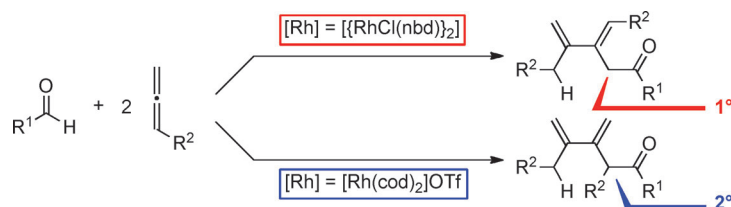
A Charge/Discharge Device for Chemical Hydrogen Storage and Generation

Coupling Reactions

T. Toyoshima, T. Miura,
M. Murakami* — 10436–10439



Selective 1:2 Coupling of Aldehydes and Allenes with Control of Regiochemistry



Counterions in control: The rhodium(I)-catalyzed coupling of one molecule of aldehyde and two molecules of allene gave β,γ -dialkylidene ketones (see scheme).

Either of two constitutional isomers was selectively obtained depending on the counterion of the rhodium(I) complex.

Actinide Photochemistry

B. M. Gardner, D. Patel, W. Lewis,
A. J. Blake, S. T. Liddle* — 10440–10443



Photochemically Promoted Bond-Cleavage and -Capture in a Diazomethane Derivative of a Triamidoamine Uranium(IV) Complex



Photolysis of $[\text{U}(\text{tren}^{\text{TM}})(\mu\text{-N}(\text{SiMe}_3)\text{-NC})_2]$ (see scheme; $\text{R} = \text{SiMe}_3$) results in multiple bond cleavage and capture to give a well-defined product

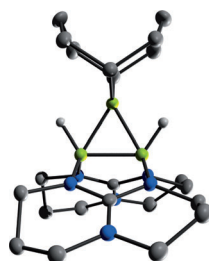
$[\text{U}\{\text{N}(\text{CH}_2\text{CH}_2\text{NSiMe}_3)_2(\mu\text{-CH}_2\text{CH}_2\text{N-C}\equiv\text{N})\}\{\text{N}(\text{SiMe}_3)_2\}_2]$. This transformation has no precedent in diazoalkane chemistry and is not thermally accessible.

Boron Triangle

N. Schulenberg, H. Wadepohl,
H.-J. Himmel* — 10444–10447



Synthesis and Characterization of a Doubly Base-Stabilized B_3H_6^+ Analogue



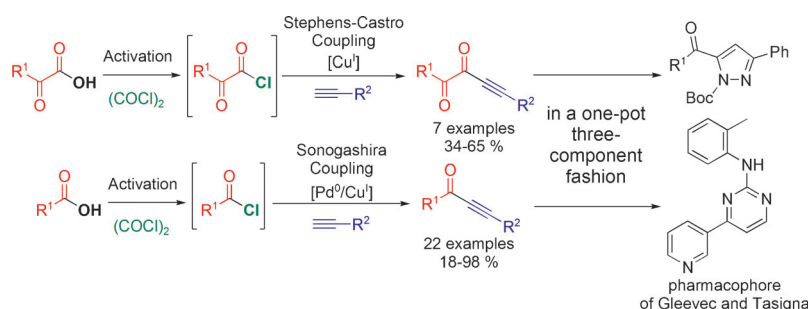
The answer to an old question: A doubly base-stabilized B_3H_6^+ analogue (see structure: B green, C gray, N blue, H light gray, H on C not shown) has been synthesized and completely characterized. Quantum-chemical calculations on a simplified model confirmed the presence of closed B-B-B three-center bonding and σ -aromatic character.

One-Pot Reactions

C. Boersch, E. Merkul,
T. J. J. Müller* — 10448–10452

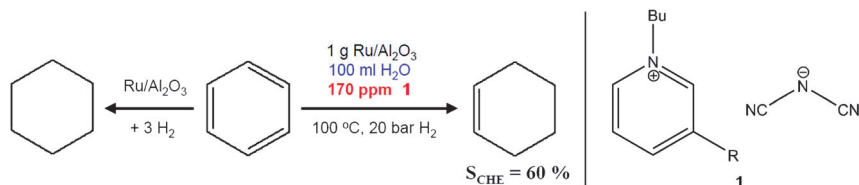


Catalytic Syntheses of N-Heterocyclic Ynones and Ynediones by In Situ Activation of Carboxylic Acids with Oxalyl Chloride



Breaking the bottleneck: α -Keto carboxylic acids and N-heterocyclic carboxylic acids are activated in situ with oxalyl chloride then catalytically alkynylated to give ynediones and N-heterocyclic ynones efficiently in a one-pot fashion. 5-Acylpyra-

zoles and 2-phenylaminopyrimidines, potentially interesting for pharmaceutical applications, are readily synthesized in concise one-pot, three-component syntheses.



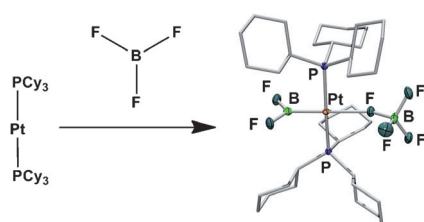
Reducing circumstances: The hydrogenation of benzene in organic phase leads rapidly to cyclohexane. A very simple catalyst system comprising only supported ruthenium in water with the addition of the ionic liquid **1** (R = Me) in the

ppm range catalyzes the extremely difficult selective hydrogenation of benzene to cyclohexene. It is not necessary to add large amounts of salt (ZnSO₄) or other metals, which is otherwise done to control selectivity.

Heterogeneous Catalysis

F. Schwab, M. Lucas,
 P. Claus* 10453 – 10456

Ruthenium-Catalyzed Selective Hydrogenation of Benzene to Cyclohexene in the Presence of an Ionic Liquid



A difficult break-up: Boron trifluoride was activated by oxidative addition to the transition-metal complex [(Cy₃P)₂Pt]. The product of this addition, *trans*-[(Cy₃P)₂Pt-(BF₂)(BF₃)], was characterized by NMR spectroscopy and crystal structure determination. Furthermore, the degradation product *trans*-[(Cy₃P)₂Pt(H)(BF₃)] and the stable derivative *trans*-[(Cy₃P)₂Pt-(BF₂)(Cl)] were fully characterized.

B–F Activation

J. Bauer, H. Braunschweig,* K. Kraft,
 K. Radacki 10457 – 10460

Oxidative Addition of Boron Trifluoride to a Transition Metal



Supporting information is available on www.angewandte.org (see article for access details).



A video clip is available as Supporting Information on www.angewandte.org (see article for access details).



This article is available online free of charge (Open Access)

Looking for outstanding employees?

Do you need another expert for your excellent team?
 ... Chemists, PhD Students, Managers, Professors, Sales Representatives...

Place an advert in the printed version and have it made available online for 1 month, free of charge!

Angewandte Chemie International Edition

Advertising Sales Department: Marion Schulz

Phone: 0 62 01 - 60 65 65

Fax: 0 62 01 - 60 65 50

E-Mail: MSchulz@wiley-vch.de

Service

**Spotlight on Angewandte's
 Sister Journals** 10278 – 10280

Preview 10461

Corrigendum

NaSr₃Be₃B₃O₉F₄: A Promising Deep-Ultraviolet Nonlinear Optical Material Resulting from the Cooperative Alignment of the [Be₃B₃O₁₂F]¹⁰⁻ Anionic Group

H. Huang, J. Yao, Z. Lin, X. Wang, R. He, W. Yao, N. Zhai, C. Chen* — **9141–9144**

Angew. Chem. Int. Ed. **2011**, 50

DOI 10.1002/anie.201103960

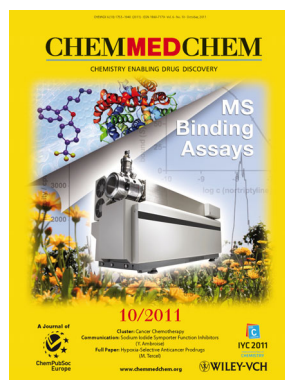
The authors of this Communication wish to add a second affiliation for Hongwei Huang, Ran He, Wenjiao Yao, and Naixia Zhai as shown below.

Graduate University of Chinese Academy of Sciences
Beijing 100049 (P. R. China)

Check out these journals:



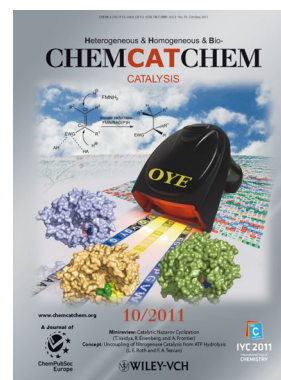
www.chemasianj.org



www.chemmedchem.org



www.chemsuschem.org



www.chemcatchem.org